Available online at www.sciencedirect.com
ScienceDirect
Dyes and Pigments 73 (2007) 269–278
DYES and PIGMENTS
www.elsevier.com/locate/dyepig

Use of bagasse fly ash as an adsorbent for the removal of brilliant green dye from aqueous solution

Venkat S. Mane, Indra Deo Mall*, Vimal Chandra Srivastava

Department of Chemical Engineering, Indian Institute of Technology Roorkee, Roorkee 247 667, India

Received 14 August 2005; received in revised form 19 October 2005; accepted 14 December 2005
Available online 15 March 2006

Abstract

The present study deals with the adsorption of brilliant green (BG) on carbon rich bagasse fly ash (BFA). BFA is a solid waste obtained from the particulate collection equipment attached to the flue gas line of the bagasse-fired boilers of cane sugar mills. Batch studies were performed to evaluate the influences of various experimental parameters like initial pH (pH_0), contact time, adsorbent dose and initial concentration (C_0) on the removal of BG. Optimum conditions for BG removal were found to be $pH_0 \approx 3.0$, adsorbent dose ≈ 3 g/l of solution and equilibrium time ≈ 5 h. Adsorption of BG followed pseudo-second-order kinetics. Intra-particle diffusion does not seem to control the BG removal process. Equilibrium isotherms for the adsorption of BG on BFA were analyzed by Freundlich, Langmuir, Redlich–Peterson, Dubnin–Radushkevich, and Temkin isotherm models using non-linear regression technique. Redlich–Peterson and Langmuir isotherms were found to best represent the data for BG adsorption onto BFA. Adsorption of BG on BFA is favourably influenced by an increase in the temperature of the operation. Values of the change in entropy (ΔS^0) and heat of adsorption (ΔH^0) for BG adsorption on BFA were positive. The high negative value of change in Gibbs free energy (ΔG^0) indicates the feasible and spontaneous adsorption of BG on BFA.

Keywords: Dye removal; Bagasse fly ash; Adsorption kinetics; Isotherms; Error analyses; Adsorption thermodynamics

1. Introduction

Due to ever-growing demands in textiles, synthetic organic dyes are widely used for dyeing textile fibers such as cotton and polyester. Approximately 10,000 different dyes and pigments are used for industries and over 7×10^5 tons of these dyes are annually produced worldwide [1]. Dyes and pigments represent one of the problematic groups; they are emitted into wastewaters from various industrial branches, mainly from the dye manufacturing and textile finishing [2] and also from food colouring, cosmetics, paper and carpet industries. Synthetic dyes have complex aromatic structures which provide them physico-chemical, thermal and optical stability [3,4]. Dyes in effluents, if not removed, cause disturbance to the ecological systems of the receiving waters. These materials also pose certain health hazards and environmental pollution. Brilliant green (BG) dye is used for the production of cover paper in the paper industry. About 0.8–1.0 kg of BG is consumed per ton of paper produced. However, BG dye causes irritation to the gastrointestinal tract, symptoms may include nausea, vomiting and diarrhea. It may cause irritation to the respiratory tract, symptoms may include coughing and shortness of breath. BG containing effluents are generated from textiles, printing and dyeing, paper, rubber, plastic industries, etc.

Activated carbons are widely used as adsorbents for the treatment of polluted water or wastewater. In these wide applications of activated carbons, adsorption property and capacity of activated carbons play an important role. Adsorption capacity of activated carbons mainly depends on pore characteristics such as specific surface area, pore size, and its distribution. Commonly, most commercially available activated carbons

* Corresponding author. Tel.: +91 1332 285319 (Office), +91 1332 285106 (Residence); fax: +91 1332 276535/3560.
E-mail address: id_mall2000@yahoo.co.in (I.D. Mall).

0143-7208/$ - see front matter © 2006 Elsevier Ltd. All rights reserved.
doi:10.1016/j.dyepig.2005.12.006

Nomenclature

$1/n$	heterogeneity factor, dimensionless
a_R	constant of Redlich–Peterson isotherm (l/mg)
BFA	bagasse fly ash
C_0	initial concentration of adsorbate in solution (mg/l)
C_e	equilibrium liquid phase concentration (mg/l)
C_s	adsorbent concentration in the solution
h	initial sorption rate (mg/g min)
HYBRID	hybrid fractional error function
I	constant that gives idea about the thickness of boundary layer (mg/g)
k_0	constant in Bangham's equation
k_f	rate constant of pseudo-first-order adsorption model (min^{-1})
k_{id}	intra-particle diffusion rate constant (mg/g $min^{1/2}$)
k_s	rate constant of pseudo-second-order adsorption model (g/mg min)
K_F	constant of Freundlich isotherm ((mg/g)/(l/mg)$^{1/n}$)
K_L	constant of Langmuir isotherm (l/mg)
K_R	constant of Redlich–Peterson isotherm (l/g)
m	mass of adsorbent per liter of solution (g/l)
n	number of data points
p	number of parameters
MPSD	Marquardt's percent standard deviation
q_e	equilibrium solid phase concentration (mg/g)
$q_{e,cal}$	calculated value of solid phase concentration of adsorbate at equilibrium (mg/g)
$q_{e,exp}$	experimental value of solid phase concentration of adsorbate at equilibrium (mg/g)
q_m	maximum adsorption capacity of adsorbent (mg/g)
q_t	amount of adsorbate adsorbed by adsorbent at time t (mg/g)
R	universal gas constant (8.314 J/K mol)
R_L	separation factor (dimensionless)
t	time (min)
T	absolute temperature (K)
V	volume of the solution (l)
w	mass of the adsorbent (g)
ΔG^0	Gibbs free energy of adsorption (kJ/mol)
ΔH^0	enthalpy of adsorption (kJ/mol)
ΔS^0	entropy of adsorption (J/K mol)

Greek symbols

α	Bangham's constant (<1)
β	constant of Redlich–Peterson isotherm ($0 < \beta < 1$)

are extremely microporous and of high surface area, and consequently they have high efficiency for the adsorption or removal of low molecular weight compounds. However, the adsorption of giant molecules exhibiting high molecular weight on microporous activated carbon is very low. Also, adsorbent-grade activated carbon is cost-prohibitive and both regeneration and disposal of the used carbon are often very difficult. Consequently, many investigators have studied the feasibility of using low cost substances for the treatment of wastewater.

The sugar industry is one of the most important agri-based industries in India, South America and Caribbean countries. Bagasse fly ash (BFA), a waste collected from the particulate collection equipment attached upstream to the stacks of bagasse-fired boilers, causes disposal problems. It is mainly used for land filling, and partly used as filler in building materials and paper and wood boards. BFA has good adsorptive properties and has been used for the removal of COD and colour from sugar mill [5] and paper mill effluents [6]. Various researchers have utilized it for the adsorptive removal of phenolic compounds [7,8] and dyes [9–11]. The aim of the present work is to explore the possibility of utilizing BFA for the adsorptive removal of BG from aqueous solution. The effect of factors such as initial pH (pH_0), adsorbent dose (m), contact time (t), initial concentration (C_0) and temperature (T) was investigated. The kinetics of BG adsorption onto BFA was analyzed by fitting various kinetic models. Experimental equilibrium data were fitted to the Freundlich, Langmuir, Redlich–Peterson (R–P), Dubnin–Radushkevich (D–R) and Temkin isotherm equations to determine the best-fit isotherm equation. Error analysis was carried out to test the adequacy and the accuracy of the model equations. The effect of temperature on BG adsorption on BFA has also been investigated. Thermodynamics of adsorption process have been studied and the change in Gibbs free energy, the enthalpy and the entropy of adsorption has also been determined.

2. Material and methods

2.1. BFA

BFA was used as obtained from a nearby sugar mill (Deoband sugar mill, U.P., India), without any pretreatment for the removal of BG from synthetic aqueous solutions in a batch treatment process. Detailed physico-chemical characteristics of the BFA have already been presented elsewhere [9–11].

2.2. Adsorbate

The adsorbate, BG dye (C.I. = 42,040, chemical formula = $C_{27}H_{34}N_2O_4S$, FW = 482.62; nature = basic green 4) was supplied by s.d. Fine Chemicals, Mumbai, India. The structure of BG is illustrated in Fig. 1. An accurately weighed quantity of the dye was dissolved in double-distilled water to prepare stock solution (1000 mg/l). Experimental solutions of the desired concentrations were obtained by successive dilutions with distilled water.

2.3. Analytical measurements

Concentrations of dyes were determined by finding out the absorbance at the characteristic wavelength using a double beam UV/vis spectrophotometer (Perkin Elmer 135). A standard solution of the dye was taken and the absorbance was

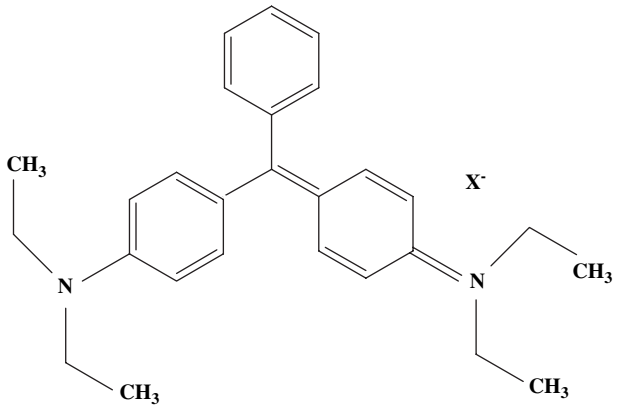

Fig. 1. Molecular structure of brilliant green.

determined at different wavelengths to obtain a plot of absorbance versus wavelength. The wavelength corresponding to maximum absorbance (λ_{max}) as determined from this plot was 623 nm. This wavelength was used for preparing the calibration curves between absorbance and the concentration of the dye solution. The calibration plot of absorbance versus concentration for BG showed a linear variation up to 20 mg/l concentration. Therefore, the samples with higher concentrations of BG (>20 mg/l) were diluted with distilled water, whenever necessary, to make the concentration less than 20 mg/l, for the accurate determination of the BG concentration with the help of the linear portion of the calibration curve.

2.4. Batch experimental programme

To study the effect of important parameters like pH_0, m, C_0 and t on the adsorptive removal of BG, batch experiments were conducted at 303 ± 1 K. For each experimental run, 50 ml of BG solution of known concentration, pH_0 and a known amount of the adsorbent were taken in a 250 ml stoppered conical flask. This mixture was agitated in a temperature-controlled orbital shaker at a constant speed of 150 rpm at 303 ± 1 K. Samples were withdrawn at appropriate time intervals. Some BFA particles remain suspended and do not settle down easily. Therefore, all the samples were centrifuged (Research Centrifuge, Remi Scientific Works, Mumbai) at 7000 rpm for 10 min and analyzed for the residual dye concentration. The effect of pH_0 on dye removal was studied over a pH_0 range of 2–11. pH_0 was adjusted by the addition of dilute aqueous solutions of HCl or NaOH (0.10 M). For the optimum amount of adsorbent per unit mass of adsorbate, a 50 ml dye solution was contacted with different amounts of BFA till equilibrium was attained. The kinetics of adsorption was determined by analyzing adsorptive uptake of the dye from the aqueous solution at different time intervals. For adsorption isotherms, BG solution of different concentrations was agitated with the known amount of adsorbent till the equilibrium was achieved. The effect of temperature on the sorption characteristics was investigated by determining the adsorption isotherms at 288, 303 and 318 K. C_0 was varied from 50 to 300 mg/l. Blank experimental runs, with only the adsorbent in 50 ml of double-distilled water, were conducted simultaneously at similar conditions to account for any colour leached by the adsorbents and adsorbed by glass containers.

3. Result and discussion

3.1. Effect of initial pH (pH_0)

pH is, also, known to affect the structural stability of brilliant green and therefore, its colour intensity. Fig. 2 shows the colour removal with and without BFA over a pH_0 range of 2–11. The effect of pH_0 was studied with blank solutions of $C_0 = 100$ mg/l having natural $pH_0 = 2.9$. The solution was kept for 1 h, after which the absorbance of the solution at $\lambda = 623$ nm was found out. It is found that the colour is stable at the natural $pH_0 = 2.9$. However, colour reduction increases as pH_0 increases with maximum colour removal at $pH_0 = 11$. Colour removal due to pH change alone may be due to the structural changes being effected in the dye molecules [9,10]. It can also be inferred from Fig. 2 that the colour removal due to adsorption of dye on BFA is maximum and constant for pH_0 greater than or equal to 2.9. Since 2.9 is the natural pH of the solution, further experiments were conducted without adjusting the pH.

3.2. Effect of adsorbent dosage (m)

The effect of m on the removal of BG by BFA at $C_0 = 100$ mg/l is shown in Fig. 3. It can be seen that the BG removal increases up to a certain limit and then it remains almost constant. An increase in the adsorption with the adsorbent dosage can be attributed to greater surface area and the availability of more adsorption sites. At $m < 2.5$ g/l, the adsorbent surface becomes saturated with BG and the residual concentration in the solution is large. With increase in the m, the BG removal increases due to increased BG uptake by the increased amount of adsorbent. At $m > 2.5$ g/l, the incremental BG removal becomes very low, as the surface BG concentration and the solution BG concentration come to equilibrium with each other. At about $m = 3$ g/l, the removal efficiency becomes almost constant.

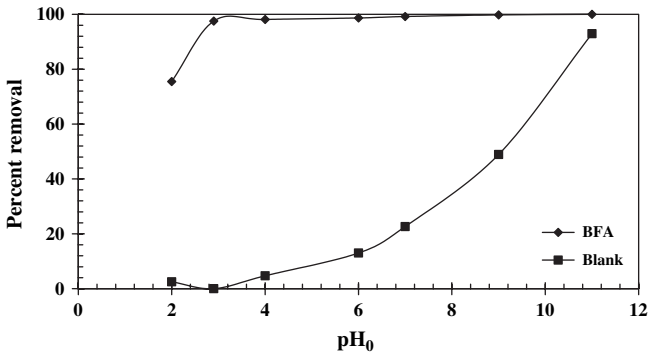

Fig. 2. Effect of pH_0 on the adsorption of BG by adsorbent as BFA ($T = 303$ K, $t = 5$ h, $C_0 = 100$ mg/l, BFA dose = 3 g/l).

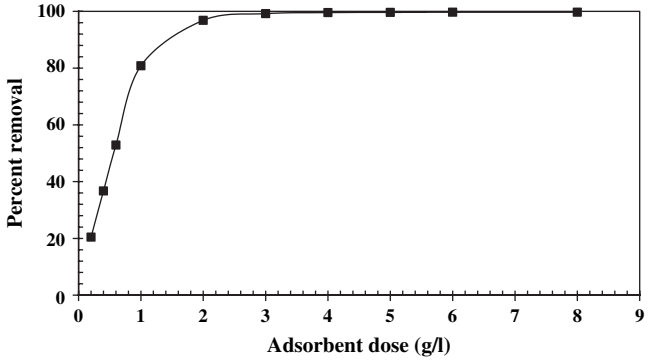

Fig. 3. Effect of adsorbent dose on the adsorption of BG by BFA ($T = 303$ K, $t = 5$ h, $C_0 = 100$ mg/l).

3.3. Effect of initial dye concentration (C_0)

The effect of C_0 on the removal of BG by BFA is shown in Fig. 4. It is evident from the figure that the amount of BG adsorbed per unit mass of BFA (q_e) increased with the increase in C_0, although percentage BG removal decreased with the increase in C_0. The C_0 provides the necessary driving force to overcome the resistances to the mass transfer of BG between the aqueous and the solid phases. The increase in C_0 also enhances the interaction between BG and BFA. Therefore, an increase in C_0 of BG enhances the adsorption uptake of BG. The rate of adsorption also increases with the increase in C_0 due to increase in the driving force.

3.4. Effect of contact time

Effect of contact time for the removal of BG by the BFA at $C_0 = 50$, 100 and 200 mg/l for $m = 3$ g/l showed rapid adsorption of dye in the first 15 min and, thereafter, the adsorption rate decreased gradually and the adsorption reached equilibrium in about 5 h as shown in Fig. 4. Increase in contact time up to 3 days showed that the BG removal by BFA was only by about 0.5% over those obtained for 5 h contact time. Aggregation of dye molecules with the increase in contact time makes it almost impossible to diffuse deeper into the adsorbent structure at highest energy sites. This aggregation

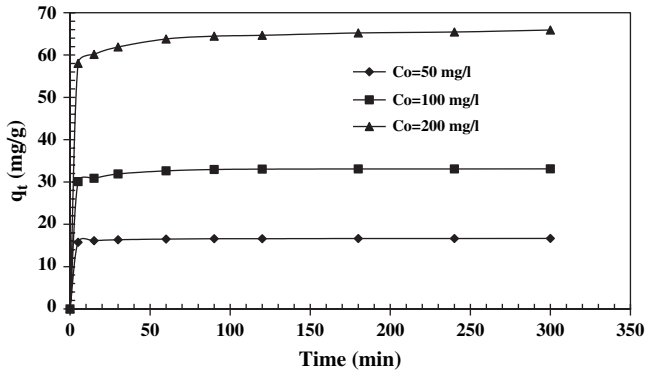

Fig. 4. Effect of contact time on the removal of BG ($T = 303$ K, $C_0 = 50$, 100 and 200 mg/l, $m = 3$ g/l).

negates the influence of contact time as the mesopores get filled up and start offering resistance to diffusion of aggregated dye molecules in the adsorbents. This is the reason why an insignificant enhancement in adsorption is effected in 7 days as compared to that in 5 h. Since the difference in the adsorption values at 5 h and at 7 days is very small, after 5 h contact, a steady-state approximation was assumed and a quasi-equilibrium situation was accepted. Further experiments were conducted for 5 h contact time only. The adsorption curves were single, smooth and continuous leading to saturation and indicated the possible mono-layer coverage on the surface of adsorbents by the dye molecules [12,13].

3.5. Adsorption kinetic study

In order to investigate the adsorption processes of BG on the BFA, pseudo-first-order, pseudo-second-order, Bangham and intra-particle diffusion kinetic models were used.

3.5.1. Pseudo-first-order model

The pseudo-first-order equation is given as:

$$\frac{dq_t}{dt} = k_f(q_e - q_t) \tag{1}$$

where q_t is the amount of adsorbate adsorbed at time t (mg/g), q_e is the adsorption capacity at equilibrium (mg/g), k_f is the pseudo-first-order rate constant (min^{-1}), and t is the contact time (min). The integration of Eq. (1) with the initial condition, $q_t = 0$ at $t = 0$ leads to [14]:

$$\log(q_e - q_t) = \log q_e - \frac{k_f}{2.303}t \tag{2}$$

The values of adsorption rate constant (k_f) for BG adsorption on RHFA were determined from the plot of $\log(q_e - q_t)$ against t (not shown here). These values ($k_f = 0.0198$, 0.0269 and 0.0152 min^{-1} for $C_0 = 50$, 100 and 200 mg l^{-1}, respectively) (Table 1) are close to values for the adsorption of BG on neem leaf powder [15] and modified peat–resin particle [16] (0.0073 and 0.0061 min^{-1}, respectively).

3.5.2. Pseudo-second-order model

The pseudo-second-order model is represented as [17]:

$$\frac{dq_t}{dt} = k_s(q_e - q_t)^2 \tag{3}$$

where k_s is the pseudo-second-order rate constant (g/mg min). Integrating Eq. (3) and noting that $q_t = 0$ at $t = 0$, the following equation is obtained:

$$q_t = \frac{tk_sq_e^2}{1 + tk_sq_e} \tag{4}$$

The initial sorption rate, h (mg/g min), at $t \to 0$ is defined as:

$$h = k_sq_e^2 \tag{5}$$

Table 1
Kinetic parameters for the removal of brilliant green by BFA ($T = 303$ K, $C_0 = 50$, 100 and 200 mg/l, $m = 3$ g/l)

Pseudo-first-order model					
C_0 (mg/l)	$q_{e,exp}$ (mg/g)	$q_{e,cal}$ (mg/g)	k_f (min^{-1})	R^2 (linear)	R^2 (non-linear)
50	16.6644	1.1762	0.0198	0.6831	−0.8260
100	33.0893	4.0086	0.0269	0.8406	−0.7471
200	65.9293	10.1391	0.0152	0.7194	−0.8449

Pseudo-second-order model					
C_0 (mg/l)	$q_{e,cal}$ (mg/g)	h (mg/g min)	k_s (g/mg min)	R^2 (linear)	R^2 (non-linear)
50	16.6666	39.2156	0.1412	1	0.9999
100	33.2225	47.6190	0.0431	1	0.9999
200	65.7894	45.4545	0.0105	0.9999	0.9993

Bangham's model				
C_0 (mg/l)	k_0 (g)	α	R_1^2 (linear)	R_2^2 (non-linear)
50	0.9225	0.2431	0.9318	0.9652
100	0.8883	0.2070	0.9587	0.9819
200	0.8535	0.1912	0.9839	0.9919

Intra-particle diffusion model				
C_0 (mg/l)	k_{id} (mg/g min$^{1/2}$)	I_1 (mg/g)	R_1^2 (linear)	R_2^2 (non-linear)
50	0.1340	15.538	0.9255	0.9620
100	0.4721	29.089	0.9820	0.9909
200	1.0428	55.929	0.9893	0.9946
C_0 (mg/l)	$k_{id,2}$ (mg/g min$^{1/2}$)	I_2 (mg/g)	R_2^2 (linear)	R_2^2 (non-linear)
50	0.0103	16.485	0.9904	0.9892
100	0.0176	32.801	0.7747	0.8468
200	0.1832	62.709	0.9874	0.9929

The q_e is obtained from the slope of the t/q_t versus t (Fig. 5) and h is obtained from the intercept. Since q_e is known from the slope, the k_s can be determined from the value of h. The best-fit values of h, q_e and k_s along with correlation coefficients for the pseudo-first-order and pseudo-second-order models are shown in Table 1. The $q_{e,exp}$ and the $q_{e,cal}$ values for the pseudo-first-order and pseudo-second-order models are also shown in Table 1. The $q_{e,exp}$ and the $q_{e,cal}$ values from the pseudo-second-order kinetic model are very close to each other. The calculated correlation coefficients are also closer to unity for pseudo-second-order kinetics than that for the pseudo-first-order kinetic model. Therefore, the sorption can be approximated more appropriately by the pseudo-second-order kinetic model than the first-order kinetic model for the adsorption of BG by BFA.

3.5.3. Bangham's equation

Bangham's equation [18] is given as:

$$\log\log\left(\frac{C_0}{C_0 - q_t m}\right) = \log\left(\frac{k_0 m}{2.303V}\right) + \alpha \log(t) \tag{6}$$

where V is the volume of the solution (ml), and α (<1) and k_0 are constants. The double logarithmic plot (not shown here), according to Eq. (6), did not yield satisfactory linear curves for the BG removal by the BFA. This shows that the diffusion of adsorbate into the pores of the sorbent was not the only rate-controlling step [19]. It may be that both the film and pore diffusion were important to different extents in the removal process.

3.5.4. Intra-particle diffusion study

The possibility of intra-particle diffusion resistance affecting adsorption was explored by using the intra-particle diffusion model [20] as:

$$q_t = k_{id} t^{1/2} + I \tag{7}$$

where k_{id} is the intra-particle diffusion rate constant. In Fig. 6, a plot of q_t versus $t^{1/2}$ is presented for adsorption of BG onto BFA. Values of I (Table 1) give an idea about the thickness of the boundary layer, i.e. the larger the intercept the greater the boundary layer effect [21]. The deviation of straight lines from the origin (Fig. 7) may be because of the difference between the rate of mass transfer in the initial and final stages of adsorption. Furthermore, such deviation of straight line from the origin indicates that the pore diffusion is not the sole rate-controlling step [22] as shown earlier by Bangham's equation. From Fig. 7, it may be seen that there are two separate regions — the initial portion is attributed to the bulk diffusion and the linear portion to intra-particle diffusion [23]. The

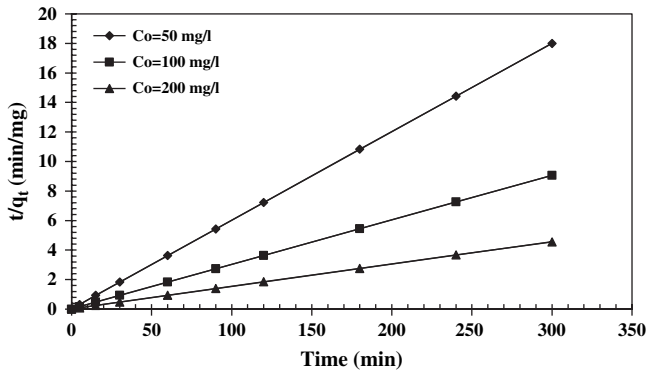

Fig. 5. Pseudo-second-order kinetic plot for the removal of BG ($T = 303$ K, $C_0 = 50$, 100 and 200 mg/l, $m = 3$ g/l).

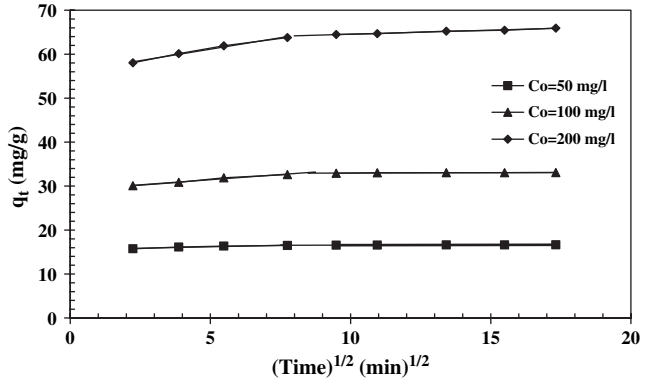

Fig. 6. Weber and Morris intra-particle diffusion plot for the removal of BG ($T = 303$ K, $C_0 = 50$, 100 and 200 mg/l, $m = 3$ g/l).

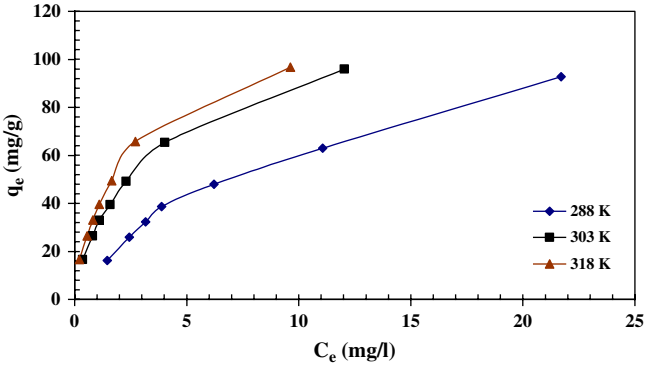

Fig. 7. Equilibrium adsorption isotherms at different temperatures for BG–BFA system ($t = 5$ h, $m = 3$ g/l).

values of $k_{id,1}$ and $k_{id,2}$ as obtained from the slopes of the two straight lines are listed in Table 1.

3.6. Effect of temperature

Temperature has a pronounced effect on the adsorption capacity of the adsorbents. Fig. 7 shows the plots of adsorption isotherms, q_e versus C_e for BG–BFA system at different temperatures (288, 303 and 318 K). It shows that with the increase in temperature, the adsorptivity of BG increases. This figure also shows that at lower adsorbate concentrations, q_e rises sharply and thereafter the increase is gradual with solute concentration in the solution. Since sorption is an exothermic process, it would be expected that an increase in temperature of the adsorbate–adsorbent system would result in decreased sorption capacity. However, if the adsorption process is controlled by the diffusion process (intra-particle transport-pore diffusion), the sorption capacity will show an increase with an increase in temperatures. This is basically due to the fact that the diffusion process is an endothermic process [24]. With an increase in temperature, the mobility of the BG ions increases and the retarding forces acting on the diffusing ions decrease, thereby increasing the sorptive capacity of adsorbent. As has been shown earlier, the diffusion of adsorbate into pores of the sorbent is not the only rate-controlling step, and the diffusion process could be ignored with adequate contact time. Therefore, the increase in sorption capacity with an increase in temperature may be attributed to chemisorption [8].

3.7. Adsorption equilibrium study

To optimize the design of an adsorption system for the adsorption of adsorbates, it is important to establish the most appropriate correlation for the equilibrium curves. Various isotherm equations like those of Freundlich, Langmuir, R–P, and Temkin have been used to describe the equilibrium characteristics of adsorption. The Freundlich isotherm [25] is derived by assuming a heterogeneous surface with a non-uniform distribution of heat of adsorption over the surface. Whereas in the Langmuir theory [26], the basic assumption is that the sorption takes place at specific homogeneous sites within the adsorbent.

The Redlich–Peterson (R–P) isotherm [27] can be described as follows:

$$q_e = \frac{K_R C_e}{1 + a_R C_e^{\beta}} \tag{8}$$

where K_R is R–P isotherm constant (l/g), a_R is R–P isotherm constant (l/mg) and β is the exponent which lies between 0 and 1, C_e is the equilibrium liquid phase concentration (mg/l).

For high concentrations, Eq. (8) reduces to Freundlich isotherm

$$q_e = K_F C_e^{1/n} \tag{9}$$

where $K_F = K_R/a_R$ is the Freundlich constant (l/mg), and $(1/n) = (1 - \beta)$ is the heterogeneity factor.

For $\beta = 1$, Eq. (8) reduces to Langmuir equation, i.e.

$$q_e = \frac{q_m K_L C_e}{1 + K_L C_e} \tag{10}$$

where K_L ($=a_R$) is the Langmuir adsorption constant (l/mg) related to the energy of adsorption and q_m ($=K_R/a_R$) signifies adsorption capacity (mg/g).

For $\beta = 0$, Eq. (8) reduces to Henry's equation, i.e.

$$q_e = \frac{K_R C_e}{1 + a_R} \tag{11}$$

The R–P isotherm incorporates three parameters and can be applied in either a homogenous or a heterogeneous system. Eq. (8) can be converted to a linear form by taking logarithms of both the sides as:

$$\ln\left(K_R \frac{C_e}{q_e} - 1\right) = \ln a_R + \beta \ln C_e \tag{12}$$

A minimization procedure has been adopted to solve Eq. (12) by maximizing the correlation coefficient between the predicted values of q_e from Eq. (12) and the experimental data using the solver add-in function of the MS excel.

The Temkin isotherm is given as:

$$q_e = \frac{RT}{b} \ln(K_T C_e) \tag{13}$$

which can be linearized as:

$$q_e = B_1 \ln K_T + B_1 \ln C_e \tag{14}$$

where

$$B_1 = \frac{RT}{b} \tag{15}$$

Temkin isotherm contains a factor that explicitly takes into the account adsorbing species–adsorbent interactions. This isotherm assumes that (i) the heat of adsorption of all the molecules in the layer decreases linearly with coverage due to adsorbent–adsorbate interactions, and that (ii) the adsorption is

characterized by a uniform distribution of binding energies, up to some maximum binding energy [28,29]. A plot of q_e versus $\ln C_e$ enables the determination of the isotherm constants B_1 and K_T from the slope and the intercept, respectively. K_T is the equilibrium binding constant (l/mol) corresponding to the maximum binding energy and constant B_1 is related to the heat of adsorption.

Another equation used in the analysis of isotherms was proposed by Dubinin and Radushkevich (D–R) [30].

$$q_e = q_s \exp(-B\varepsilon^2) \tag{16}$$

where q_s is the D–R constant and ε can be correlated as:

$$\varepsilon = RT \ln\left(1 + \frac{1}{C_e}\right) \tag{17}$$

The constant B gives the mean free energy E of sorption per molecule of sorbate when it is transferred to the surface of the solid from infinity in the solution and can be computed using the following relationship [31]:

$$E = \frac{1}{\sqrt{2B}} \tag{18}$$

Freundlich, Langmuir, R–P, Temkin and D–R isotherm constants were determined from the plots of $\ln q_e$ versus $\ln C_e$, C_e/q_e versus C_e (Fig. 8), $K_R C_e/q_e$ versus $\ln C_e$ (Fig. 9), q_e versus $\ln C_e$, and $\ln q_e$ versus ε^2, respectively, at 15, 30 and 45 °C using MS Excel for Windows. It was found that the R–P isotherm best represents the equilibrium adsorption of BG on BFA at 303 and 318 K, whereas, Langmuir isotherm best followed the equilibrium adsorption data at 288 K. The isotherm constants for all the isotherms studied, and the correlation coefficient, R^2 with the experimental data are listed in Table 2. The correlation coefficients for R–P isotherm are highest in comparison to the values obtained for the Langmuir, Freundlich, and the Temkin isotherms. Therefore, R–P is the best-fit isotherm equation for the adsorption of BG on BFA. Similar Langmuir and Freundlich constant values have been reported for adsorption of BG on neem leaf powder [15] and modified peat–resin particle [16]. Values of $1/n$ less than 1 show the favourable nature of adsorption of BG on BFA [32].

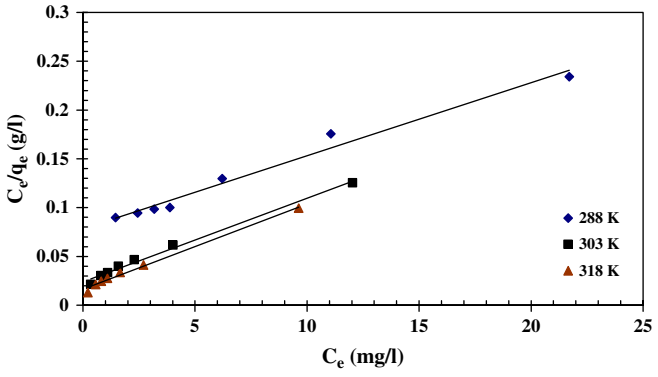

Fig. 8. Langmuir isotherm plots for the removal of BG ($t = 5$ h, $m = 3$ g/l).

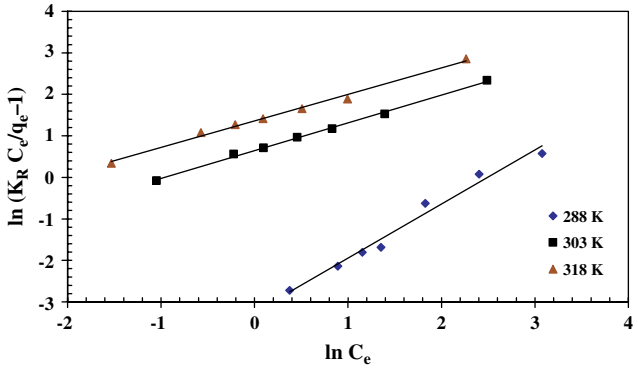

Fig. 9. Redlich–Peterson isotherm plot for the removal of BG ($t = 5$ h, $m = 3$ g/l).

3.8. Error analysis

Five different error functions of non-linear regression basin were employed in this study to find out the most suitable kinetic and isotherm models to represent the experimental data. These error functions are given in Table 3. Most

Table 2
Isotherm parameters for the removal of brilliant green by BFA ($T = 5$ h, $C_0 = 50$–300 mg/l, $m = 3$ g/l)

Freundlich constants				
T (K)	K_F ((mg/g)/(mg/l)$^{1/n}$)	$1/n$	R_1^2 (linear)	R_2^2 (non-linear)
288	14.8324	0.6164	0.9759	0.9878
303	30.2978	0.5042	0.9863	0.9931
318	36.5027	0.4797	0.9831	0.9915

Langmuir constants					
T (K)	K_L (l/mg)	q_m (mg/g)	R_L	R_1^2 (linear)	R_2^2 (non-linear)
288	0.0954	133.3333	0.09453	0.9800	0.9899
303	0.3540	116.2791	0.02725	0.9917	0.9958
318	0.5287	114.7598	0.01861	0.9917	0.9958

Redlich–Peterson constants					
T (K)	K_R (l/g)	a_R (l/mg)$^{1/\beta}$	β	R_1^2 (linear)	R_2^2 (non-linear)
288	13.1127	0.0387	0.9908	0.9796	0.9862
303	91.5453	1.9348	0.6660	0.9974	0.9987
318	186.7539	3.9394	0.6383	0.9930	0.9965

Temkin constants				
T (K)	K_T (l/mg)	B_1	R_1^2 (linear)	R_2^2 (non-linear)
288	1.0582	27.587	0.9644	0.9875
303	4.2398	23.108	0.9719	0.9858
318	6.6858	22.079	0.9752	0.9820

Dubnin–Radushkevich constants				
T (K)	q_s (mg/g)	E (kJ/mol)	R_1^2 (linear)	R_2^2 (non-linear)
288	60.7034	0.7222	0.8218	−0.9065
303	59.1159	1.9892	0.7629	−0.8734
318	59.2817	2.6744	0.7526	−0.8675

Table 3
Different error functions used for kinetic model and equilibrium isotherm analyses

Error function	Abbreviation	Formula	Reference
The sum of the squares of the errors	SSE	$\sum_{i=1}^{n}\left(q_{e,cal}-q_{e,meas}\right)_i^2$	–
The sum of the absolute errors	SAE	$\sum_{i=1}^{n}\left\|q_{e,cal}-q_{e,meas}\right\|_i$	–
The average relative error	ARE	$\frac{100}{n}\sum_{i=1}^{n}\left\|\frac{\left(q_{e,meas}-q_{e,cal}\right)}{q_{e,meas}}\right\|_i$	[33]
The hybrid fractional error function	HYBRID	$\frac{100}{n-p}\sum_{i=1}^{n}\left[\frac{\left(q_{e,meas}-q_{e,cal}\right)}{q_{e,meas}}\right]_i$	[34]
Marquardt's percent standard deviation	MPSD	$100\sqrt{\frac{1}{n-p}\sum_{i=1}^{n}\left(\frac{\left(q_{e,meas}-q_{e,cal}\right)}{q_{e,meas}}\right)_i^2}$	[35]

commonly used sum of the squares of the errors (SSE) function has a major drawback in that it provides isotherm parameters showing a better fit at the higher end of the adsorbate concentration. This is because the magnitude of the errors and hence the square of the errors increases as the adsorbate concentration increases. Isotherm parameters determined using sum of the absolute errors (SAE) method provide a better fit as the magnitude of the errors increase, biasing the fit towards the high concentration data. The average relative error (ARE) [33] function attempts to minimise the fractional error distribution across the entire concentration range. The hybrid fractional error function (HYBRID) was developed [34] in order to improve the fit of the SSE method at low concentration values by dividing by the measured value. In addition, a divisor was included as a term for the number of degrees of freedom for the system – the number of data points (n) minus the number of parameters (p) within the isotherm equation. Marquardt's percent standard deviation (MPSD) error function [35] has been used previously by a number of researchers in the field [9–11,36,37]. It is similar in some respects to a geometric mean error distribution modified according to the number of degrees of freedom of the system.

Table 4
Values of five different error analyses of isotherm models for adsorption of brilliant green by BFA ($t = 5$ h, $C_0 = 50$–300 mg/l, $m = 3$ g/l)

	SSE	SAE	ARE	HYBRID	MPSD
288 K					
Freundlich	78.6861	19.8630	7.0042	−0.4914	9.9699
Langmuir	**50.7395**	14.8018	4.2123	0.7464	5.8416
R–P	51.3035	**14.5182**	**4.0896**	**−0.6395**	**5.6378**
D–R	1253.3130	64.9181	19.1001	−0.7693	24.6346
Temkin	99.3609	21.1152	7.7887	2.3567	13.3131
303 K					
Freundlich	137.3852	22.0446	5.8359	−0.2818	7.6044
Langmuir	40.7003	14.7777	6.3095	2.2366	10.926
R–P	**18.4413**	**8.42891**	**2.2478**	**−0.0496**	**3.1544**
D–R	1909.1040	88.5399	26.7854	−17.1185	35.7287
Temkin	121.9218	24.9814	11.8829	3.3160	21.4366
318 K					
Freundlich	190.4465	24.8317	6.0024	−0.3464	8.3513
Langmuir	**53.2500**	15.7764	7.4973	1.7599	14.0562
R–P	62.3075	**15.0905**	**4.0582**	**−0.1163**	**5.7668**
D–R	1727.6830	77.9865	22.9690	2.5119	29.8075
Temkin	157.8661	30.3232	14.4266	3.3740	24.9226

The values of the error functions are presented in Table 4. By comparing the results of the values of the error functions, it is found that R–P model best-fits the BG adsorption isotherm data for the BFA at all temperatures. It may, however, be noted that the non-linear correlation coefficients, R^2 and the error analysis values are similar for the Langmuir and R–P isotherms and hence any one of the isotherms could be used for BG adsorption on BFA.

3.9. Estimation of thermodynamic parameters

The Gibbs free energy change of the adsorption process is related to the equilibrium constant by the classic Van't Hoff equation

$$\Delta G^0 = -RT\ln K \tag{19}$$

According to thermodynamics, the Gibbs free energy change is also related to the entropy change and heat of adsorption at constant temperature by the following equation:

$$\Delta G^0 = \Delta H^0 - T\Delta S^0 \tag{20}$$

Combining the above two equations, we get

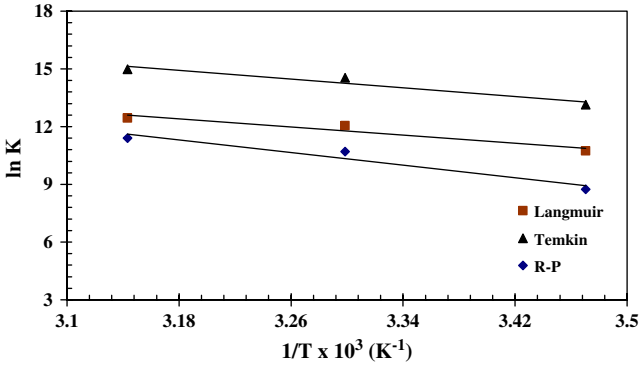

Fig. 10. Van't Hoff plot for the adsorption of BG onto BFA.

Table 5
Thermodynamic parameters adsorption of brilliant green by BFA ($t = 5$ h, $C_0 = 50$–300 mg/l, $m = 3$ g/l)

Isotherm	ΔG^0 (kJ/mol K)			ΔH^0 (kJ/mol)	ΔS^0 (J/mol K)
	288 K	303 K	318 K		
Freundlich	−26.0507	−29.6809	−33.3111	43.6851	242.0122
Langmuir	−40.7408	−43.9204	−47.1001	20.3394	211.9737
R–P	−37.7247	−43.3488	−48.9728	70.3132	374.9364

$$\ln K = \frac{-\Delta G^0}{RT} = \frac{\Delta S^0}{R} - \frac{\Delta H^0}{R}\frac{1}{T} \tag{21}$$

where ΔG^0 is the free energy change (kJ/mol), ΔH^0 is the change in enthalpy (kJ/mol), ΔS^0 is the entropy change (kJ/mol K), T is the absolute temperature (K) and R is the universal gas constant (8.314 J/mol K). Thus ΔH^0 can be determined by the slope of the linear Van't Hoff plot i.e. as $\ln K$ versus $(1/T)$, using equation:

$$\Delta H^0 = \left[R\frac{\mathrm{d}\ln K}{\mathrm{d}(1/T)}\right] \tag{22}$$

ΔH^0 obtained here corresponds to isosteric heat of adsorption ($\Delta H_{st,0}$) with zero surface coverage (i.e. $q_e = 0$) [38]. Fig. 10 shows the Van't Hoff's plot for Freundlich, Langmuir and Redlich–Peterson isotherms, from which $\Delta H_{st,0}$ and ΔS^0 values have been obtained (Table 5). For significant adsorption to occur, the free energy changes of adsorption, ΔG^0, must be negative. The thermodynamics relation between ΔG^0, ΔH^0 and ΔS^0 suggests that either (i) ΔH^0 is positive and ΔS^0 is positive and that the value of $T\Delta S$ is much larger than ΔH^0, or (ii) ΔH^0 is negative and ΔS^0 is positive or that the value of ΔH^0 is more than $T\Delta S$. BG adsorption is endothermic in nature, giving a positive value of ΔH^0. Hence, ΔS^0 has to be positive and that the positive value of $T\Delta S$ has to be larger than ΔH^0. The positive ΔH^0 value confirms the endothermic nature of the overall-sorption process. The adsorption process in the solid–liquid system is a combination of two processes: (a) the desorption of the molecules of solvent (water) previously adsorbed, and (b) the adsorption of adsorbate species. The BG ions have to displace more than one water molecule for their adsorption and this results in the endothermicity of the adsorption process. Therefore, the ΔH^0 will be positive. The positive value of ΔS^0 suggests increased randomness at the solid/solution interface with some structural changes in the adsorbate and adsorbent and an affinity of the BFA towards BG. Also, positive ΔS^0 value corresponds to an increase in the degree of freedom of the adsorbed species [8,39]. ΔG^0 values were negative indicating that the sorption process led to a decrease in Gibbs free energy. Negative ΔG^0 indicates the feasibility and spontaneity of the adsorption process.

4. Conclusion

The present study shows that the bagasse fly ash (BFA) is an effective adsorbent for the removal of BG from aqueous solution. Higher percentage of BG removal by BFA, was possible provided that the C_0 in the solution was low. Optimum adsorbent dose was ≈ 3 g/l of solution. The equilibrium between the adsorbate in the solution and on the adsorbent surface was practically achieved in 5 h. Adsorption kinetics was found to follow second-order rate expression. Equilibrium adsorption data for BG on BFA were best represented by the Redlich–Peterson and Langmuir isotherms. Adsorption of BG on BFA is favourably influenced by an increase in the temperature of the operation. The negative value of ΔG^0_{ads} indicates spontaneous adsorption of BG on BFA. Overall, BFA showed excellent adsorptive characteristics for the removal of BG from aqueous solution.

Acknowledgement

Authors are thankful to the Ministry of Human Resource and Development, Government of India, for providing financial support to undertake the work.

References

[1] Zollinger H. Color chemistry synthesis, properties and applications of organic dyes and pigments. New York: VCH Publishers; 1987. p. 92–102.
[2] Janos P, Buchtova H, Ryznarova M. Sorption of dyes from aqueous solutions onto fly ash. Water Res 2003;37:4938–44.
[3] Mckay G, Allen SJ, Meconney IF, Ottrburn MS. Transport processes in the sorption of colored ions by peat particles. J Colloid Interface Sci 1981;80(2):323–39.
[4] Seshadri S, Bishop PL, Agha AM. Anaerobic/aerobic treatment of selected azo dyes in wastewater. Waste Manage 1994;15:127–37.
[5] Mall ID, Mishra N, Mishra IM. Removal of organic matter from sugar mill effluent using bagasse flyash activated carbon. Res Ind 1994;39(6):115–9.
[6] Srivastava VC, Mall ID, Mishra IM. Treatment of pulp and paper mill wastewaters with poly aluminium chloride and bagasse fly ash. Colloid Surf A 2005;260:17–28.
[7] Mall ID, Tewari S, Singh N, Mishra IM. Utilisation of bagasse fly ash and carbon waste from fertiliser plant for treatment of pyridine and 3-picoline bearing wastewater. Proceeding of the 18th International Conference on "Solid Waste Technology and Management", held at Philadelphia, PA, USA, March 23–26, 2003.
[8] Srivastava VC, Prasad B, Mall ID, Mahadevswamy M, Mishra IM. Adsorptive removal of phenol by bagasse fly ash and activated carbon: equilibrium, kinetics and thermodynamics. Colloid Surf A 2006;272:89–104.
[9] Mall ID, Srivastava VC, Agarwal NK, Mishra IM. Adsorptive removal of malachite green dye from aqueous solution by bagasse fly ash and activated carbon-kinetic study and equilibrium isotherm analyses. Colloid Surf A 2005;264:17–28.
[10] Mall ID, Srivastava VC, Agarwal NK, Mishra IM. Removal of Congo red from aqueous solution by bagasse fly ash and activated carbon: kinetic study and equilibrium isotherm analyses. Chemosphere 2005;61:492–501.
[11] Mall ID, Srivastava VC, Agarwal NK. Removal of orange-G and methyl violet dyes by adsorption onto bagasse fly ash – kinetic study and equilibrium isotherm analyses. Dyes Pigments 2006;69:210–23.
[12] Wong Y, Yu J. Laccase catalysed decolorisation of synthetic dyes. Water Res 1999;33(16):3512–20.
[13] Malik PK. Use of activated carbons prepared from sawdust and rice-husk for adsorption of acid dyes: a case study of acid yellow 36. Dyes Pigments 2003;56:239–49.

[14] Lagergren S. About the theory of so called adsorption of soluble substances. Ksver Veterskapsakad Handl 1898;24:1–6.
[15] Bhattacharyya KG, Sarma A. Adsorption characteristics of the dye, brilliant green, on neem leaf powder. Dyes Pigments 2003;57:211–22.
[16] Sun Q, Yang L. The adsorption of basic dyes from aqueous solution on modified peat resin particle. Water Res 2003;37:1535–44.
[17] Ho YS, McKay G. Pseudo-second order model for sorption processes. Process Biochem 1999;34:451–65.
[18] Aharoni C, Sideman S, Hoffer E. Adsorption of phosphate ions by colloid ion-coated alumina. J Chem Technol Biotechnol 1979;29: 404–12.
[19] Tutem E, Apak R, Unal CF. Adsorptive removal of chlorophenols from water by bituminous shale. Water Res 1998;32:2315–24.
[20] Weber Jr WJ, Morris JC. Kinetics of adsorption on carbon from solution. J Sanit Eng Div ASCE 1963;89(SA2):31–59.
[21] Kannan K, Sundaram MM. Kinetics and mechanism of removal of methylene blue by adsorption on various carbons – a comparative study. Dyes Pigments 2001;51:25–40.
[22] Poots VJP, McKay G, Healy JJ. Removal of basic dye from effluent using wood as an adsorbent. J Water Pollut Control Fed 1978;50:926–39.
[23] Allen SJ, Mckay G, Khader KYH. Intraparticle diffusion of a basic dye-during adsorption onto sphagnum peat. Environ Pollut 1989;56:39–50.
[24] Weber Jr WJ. Physicochemical processes for water quality control. New York: Wiley-Interscience; 1972. p. 206.
[25] Freundlich HMF. Over the adsorption in solution. J Phys Chem 1906;57:385–471.
[26] Langmuir I. The adsorption of gases on plane surfaces of glass, mica and platinum. J Am Chem Soc 1918;40:1361–403.
[27] Redlich O, Peterson DL. A useful adsorption isotherm. J Phys Chem 1959;63:1024–6.
[28] Temkin MJ, Pyzhev V. Acta Physicochim URSS 1940;12:217–22.
[29] Kim Y, Kim C, Choi I, Rengraj S, Yi J. Arsenic removal using mesoporous alumina prepared via a templating method. Environ Sci Technol 2004;38:924–31.
[30] Dubinin MM, Radushkevich LV. Equation of the characteristic curve of activated charcoal. Chem Zent 1947;1:875.
[31] Hasany SM, Chaudhary MH. Sorption potential of Hare river sand for the removal of antimony from acidic aqueous solution. Appl Radiat Isot 1996;47:467–71.
[32] Faust SD, Aly OM. Adsorption processes for water treatment. Butterworths; 1987.
[33] Kapoor A, Yang RT. Correlation of equilibrium adsorption data of condensable vapours on porous adsorbents. Gas Sep Purif 1989;3(4):187–92.
[34] Porter JF, McKay G, Choy KH. The prediction of sorption from a binary mixture of acidic dyes using single- and mixed isotherm variants of the ideal adsorbed solute theory. Chem Eng Sci 1999;54:5863–85.
[35] Marquardt DW. An algorithm for least-squares estimation of nonlinear parameters. J Soc Ind Appl Math 1963;11:431–41.
[36] Ng JCY, Cheung WH, McKay G. Equilibrium studies for the sorption of lead from effluents using chitosan. Chemosphere 2003;52:1021–30.
[37] Wong YC, Szeto YS, Cheung WH, McKay G. Adsorption of acid dyes on chitosan – equilibrium isotherm analyses. Process Biochem 2004;39:693–702.
[38] Suzuki M, Fujii T. Concentration dependence of surface diffusion coefficient of propionic acid in activated carbon particles. AIChE J 1982;28:380–5.
[39] Raymon C. Chemistry: thermodynamic. Boston: McGraw-Hill; 1998. p. 737.